Bulletin of the Geological Survey of Japan, vol. 65 (3/4), p. 23 - 36, 2014

Article

Variation of mineralogical compositions in sequential extraction procedure adapted to geochemical reference materials (sediment series)

Atsuyuki Ohta[1,*], Ran Kubota[1], Takashi Okai[1]

Atsuyuki Ohta and Ran Kubota and Takashi Okai (2014) Variation of mineralogical compositions in sequential extraction procedure adapted to geochemical reference materials (sediment series). *Bull. Geol. Surv. Japan*, vol. 65 (3/4), p. 23-36, 6 figures, 3 table.

Abstract: We have applied the sequential extraction procedure developed by the Community Bureau of Reference (BCR) to eight Japanese geochemical reference materials. By using this method, we attempt to extract exchangeable and carbonate phases in step 1, extract iron hydroxide and manganese oxide in step 2, and extract metal sulfide and organic material in step 3. We use X-ray diffractometry (XRD) to measure untreated samples and the residue of samples after each step of the extraction process to determine whether the target material is satisfactorily decomposed during the procedure. For JSd-1 and JSd-3, XRD patterns do not change significantly by using the BCR procedure. Actually, most of the elements in these materials are scarcely extracted by BCR scheme. The peaks of calcite in JSd-4, JMs-1 and JMs-2 disappear in the XRD patterns after the first extraction procedure. The result suggests that the target phase of step 1 process is fully decomposed. JLk-1 and JMs-2 show high concentrations of the Fe and Mn extracted in step 2. However, it is difficult to clearly confirm the full decomposition of iron hydroxide and manganese oxide in step 2 because these materials do not show distinct peaks in the XRD patterns. Pyrite in JMs-1 disappears in step 3 of the extraction, which suggests that sulfide is satisfactorily decomposed in this process. X-ray reflection intensities of some peaks for quartz and plagioclase in JSO-1 increase significantly after step 3 of the extraction. It is assumed that organic material thickly covered the mineral surfaces and reduced the X-ray reflection from the minerals prior to the third procedure. Although this evidence is indirect, we conclude that organic material is successfully decomposed and removed from the mineral surface during the third extraction procedure. On the basis of these results, it is confirmed that the BCR protocol can properly extract target materials from the geochemical reference materials.

Keywords: geochemical reference material, sequential extraction, BCR protocol, X-ray diffractometry, speciation

1. Introduction

The Geological Survey of Japan, National Institute of Advanced Industrial Science and Technology (AIST), conducted nationwide geochemical mapping both on land and in a marine environment (Imai *et al*., 2004, 2010). These maps provide the spatial distribution of elemental concentrations on the earth's surface for environmental assessment. However, because physic-chemical properties and toxicities of elements in the materials change according to their chemical species, elemental speciation in materials must be obtained to conduct more appropriate risk assessment. A sequential extraction method widely used to identify chemical species in sediment and in soil materials has been standardized by the Community Bureau of Reference (BCR) (Crosland *et al*., 1993; Ure *et al.*, 1993), which provides reference material for quality control of sequential extraction procedures (BCR-701: lake sediment) (e.g., Sutherland, 2010). Geochemical mapping is conducted by using various sample media such as soil, regolith, and drainage system sediment (Darnley *et al*., 1995). Therefore, a wide variety of reference material should be prepared for quality control of speciation studies. For such a purpose, Kubota *et al.*

[1] AIST, Geological Survey of Japan, Institute of Geology and Geoinformation
*Corresponding author: A.Ohta, Central 7,1-1-1 Higashi, Tsukuba, Ibaraki 305-8567, Japan. Email: a.ohta@aist.go.jp

Table 1 List of eight geochemical reference materials provided by Geological Survey of Japan, AIST

Name	Category	Na (wt. %)	Mg (wt. %)	Al (wt. %)	Si (wt. %)	P (wt. %)	K (wt. %)	Ca (wt. %)	Mn (wt. %)	Fe (wt. %)	Total C (wt. %)	Total S (wt. %)	Cl (wt. %)	Ref.
JLk-1	Lake sediment	0.78	1.05	8.85	26.72	0.091	2.33	0.49	0.206	4.85	1.503	0.1052	n.d.	a, b
JSO-1	Soil	0.50	1.27	9.56	17.94	0.209	0.28	1.82	0.153	7.96	8.91	0.2	n.d.	c
JSd-1	Stream sediment	2.02	1.09	7.75	31.11	0.053	1.81	2.17	0.072	3.54	0.111	0.0068	0.00675	b, d
JSd-2	Stream sediment	1.81	1.65	6.51	28.41	0.046	0.95	2.61	0.093	8.15	0.316	1.31	0.0028	b, d
JSd-3	Stream sediment	0.30	0.71	5.24	35.53	0.036	1.64	0.40	0.115	3.06	0.62	0.06	0.0039	b, d
JSd-4	Stream sediment	1.69	2.44	7.00	23.90	0.196	1.16	3.98	0.083	5.64	2.896	1.1489	n.d.	e, f
JMs-1	Marine sediment	3.02	1.73	8.37	25.12	0.079	1.86	1.52	0.079	4.83	1.69	1.32	2.69	c
JMs-2	Marine sediment	4.30	1.95	7.50	19.53	0.550	2.24	3.34	1.75	7.67	0.39	0.29	4.05	c

a) Ando *et al*. (1990); b) Imai *et al*. (1996); c) Terashima *et al*. (2002); d) Terashima *et al*. (1990); e) Certificate of GSJ CRM JSd-4; f) Kubota (2009)

(2014) applied the BCR protocol to eight series of Japanese geochemical sedimentary reference materials. However, this method extracts various elemental forms by using chemical reagents. In some cases, a reagent extracts only a part of the targeted phase or decomposes an unintended phase (e.g., Martin *et al*., 1987; Coetzee *et al*., 1995). Thus, X-ray diffraction (XRD) analysis is used to elucidate the adequateness of the BCR protocol. The objectives of this study are to examine the manner in which the mineralogical composition of the geochemical reference material changes during the sequential extraction procedure and to compare the variation of mineralogical compositions to concentrations of elements extracted. The methods for these objectives are based on BCR protocol.

2. Sample materials

The eight series of the Japanese geochemical sedimentary reference materials were used for the sequential extraction study. JLk-1 is muddy sediment occurring 63 m below the surface of Lake Biwa (Ando *et al.*, 1990). The surface part of the sediments (uppermost 0–20 cm) was used for the production of JLk-1. JSO-1 contains Kuroboku soils (Andosol) collected from the Kanto region that originated from volcanic ash and is rich in organic materials (Terashima *et al*., 2002). JMs-1 is muddy inner bay sediment from Tokyo Bay that has anoxic facies (Terashima *et al*., 2002). The bottom sediment (0–2 m) including a small amount of shell fragments was collected for the production of JMs-1. JMs-2 is a composite material of pelagic sediments obtained from the South Pacific Ocean (Terashima *et al*., 2002). Biogenic calcareous and siliceous materials are not abundant in these sediments because the sampling locations are below the calcium carbonate compensation depth and are not in the high biogenic productivity zone (Nishimura and Saito, 1994). JSd-1–4 are stream sediment materials collected from drainage basins containing granitic rocks (JSd-1), metamorphic rocks associated with a Cu mine (JSd-2), accretionary complexes associated with chert (JSd-3), and an alluvial basin associated with an urban area (JSd-4) (e.g., Terashima *et al.*, 1990). Table 1 summarizes the concentrations of Na, Mg, Al, Si, P, K, Ca, Mn, Fe, C, S, and Cl in the eight geochemical reference materials.

3. Analytical methods

3.1 Sequential extraction procedure (BCR protocol)

Sequential extraction was performed according to the BCR scheme proposed by Rauret *et al*. (1999). The actual extraction procedure has been carefully summarized by Kubota *et al*. (2014). The BCR scheme divides elemental binding forms into four associations. In step 1, the carbonate and exchangeable phases, elements in the carbonate form and those weakly adsorbed on mineral surfaces are extracted by using acetic acid at 0.11 mol L^{-1} concentration. In step 2, the reducible phase, the elements bound to iron hydroxide and manganese oxide are extracted by using hydroxylamine hydrochloride at 0.5 mol L^{-1} concentration. In step 3, the oxidizable phase, metal sulfide and elements bound to organic matter are extracted by using hydrogen peroxide and ammonium acetate. The final residue is decomposed by using an $HF–HNO_3–HClO_4$ solution. Although the decomposition of final residue is not part of the original BCR extraction scheme, it is termed "step 4" in this study (Kubota *et al*., 2014). The concentrations of 38 elements extracted in each step were measured by using inductively coupled plasma atomic emission (ICP–AES) and ICP–mass spectroscopy (MS; Kubota *et al*. 2014). Table 2 summarizes the concentrations of the Na, Mg, Al, P, K, Ca, Mn, and Fe extracted in each step.

3.2 X-ray diffractometry

For XRD analysis, the residues from respective steps of the

Table 2 Concentrations of major elements in steps 1–4 obtained from BCR extraction procedure (Kubota *et al*., 2014)

	Na (wt. %)	Mg (wt. %)	Al (wt. %)	P (mg/kg)	K (wt. %)	Ca (wt. %)	Mn (mg/kg)	Fe (wt. %)
JLk-1	0.0066	0.029	0.022	4.3	0.026	0.145	1260	0.029
JSO-1	0.0079	0.029	0.22	4.5	0.022	0.520	140	0.0077
JSd-1	0.024	0.035	0.13	3.5	0.027	0.110	92	0.032
JSd-2	0.027	0.056	0.10	21	0.027	0.80	151	0.46
JSd-3	0.003	0.010	0.11	2.9	0.026	0.062	190	0.0023
JSd-4	0.75	0.65	0.069	8.1	0.118	2.57	179	0.037
JMs-1	1.86	0.36	0.080	6.0	0.221	0.61	159	0.034
JMs-2	2.69	0.47	0.031	73	0.225	1.14	368	0.0004
25023*	1.80	0.36	0.043	29	0.180	0.62	370	0.021

*Ohta *et al* . (2007)

Step 2

	Na (wt. %)	Mg (wt. %)	Al (wt. %)	P (mg/kg)	K (wt. %)	Ca (wt. %)	Mn (mg/kg)	Fe (wt. %)
JLk-1	0.0013	0.067	0.37	450	0.027	0.076	361	1.44
JSO-1	0.0008	0.042	1.69	52	0.006	0.066	613	0.61
JSd-1	0.008	0.082	0.38	293	0.035	0.094	99	0.41
JSd-2	0.023	0.13	0.41	261	0.049	0.52	174	1.83
JSd-3	0.0005	0.008	0.28	39	0.014	0.020	268	0.22
JSd-4	0.021	0.63	1.03	386	0.061	0.225	173	1.40
JMs-1	0.049	0.20	0.75	272	0.112	0.13	135	0.91
JMs-2	0.47	0.22	0.75	1990	0.63	0.95	14780	1.55

Step 3

	Na (wt. %)	Mg (wt. %)	Al (wt. %)	P (mg/kg)	K (wt. %)	Ca (wt. %)	Mn (mg/kg)	Fe (wt. %)
JLk-1	0.004	0.047	0.15	97	0.010	0.031	102	0.11
JSO-1	0.002	0.025	1.74	165	0.003	0.013	99	0.45
JSd-1	0.010	0.034	0.07	44	0.012	0.072	26	0.016
JSd-2	0.009	0.037	0.14	109	0.004	0.036	27	0.52
JSd-3	0.002	0.006	0.11	10	0.006	0.008	43	0.032
JSd-4	0.012	0.14	0.51	210	0.011	0.054	45	0.16
JMs-1	0.020	0.089	0.37	73	0.009	0.056	89	0.44
JMs-2	0.024	0.10	0.63	620	0.18	0.057	363	0.022

Step 4

	Na (wt. %)	Mg (wt. %)	Al (wt. %)	P (mg/kg)	K (wt. %)	Ca (wt. %)	Mn (mg/kg)	Fe (wt. %)
JLk-1	0.80	0.77	4.90	440	1.96	0.13	365	2.96
JSO-1	0.48	1.13	3.34	1790	0.20	1.08	640	6.15
JSd-1	2.11	0.90	4.23	239	1.62	1.69	542	2.75
JSd-2	1.75	1.39	3.40	281	0.80	0.98	545	4.65
JSd-3	0.32	0.67	3.56	367	1.35	0.22	697	2.71
JSd-4	0.96	0.91	3.11	1200	0.82	0.75	409	3.63
JMs-1	1.03	1.00	4.10	427	1.29	0.41	351	3.16
JMs-2	0.73	1.14	4.14	2880	1.02	1.03	507	5.57

BCR extraction applied to duplicated samples were filtrated by using a 0.45 μm cellulose–acetate membrane filter. The samples on the filters were washed five times with deionized water and were then freeze-dried. Samples with no treatment were also prepared for comparison. Each sample was characterized in the 2θ = 5°–70° range by a powder diffractometer (Rigaku RINT-2500) with CuKα radiation. The X-ray tube was operated at 40 kV with a 100 mA current. The scanning velocity was 2° (2θ) /min. Each sample was placed in a concave region (15 mm × 20 mm × 0.2 mm) of a reflection-free sample holder and was pressed vertically by using a glass microscope slide to planarize the surface and to remove excess sample powder. The detection limit for identification of unknown crystalline materials using by XRD was at least a few percentages of each sample.

BCR protocol extracts metals bound to iron hydroxide and manganese oxide at the extraction of step 2. However, these materials produced very broad diffraction peaks (halo) rather than distinct peaks in the XRD patterns at 20°–30° (2θ). Therefore, the degree of crystallization was useful for elucidating the decomposition of iron hydroxide and manganese oxide after step 2 of the extraction. The degree of crystallization (%) is calculated by the following equation in the range of 10°–40° (2θ) after removal of background scattering unrelated to amorphous and crystalline materials:

$$\text{degree of crystallization } (\%) = 100 \times I_c / (I_c + I_a),$$

where I_c and I_a indicate the integrated intensity of all crystalline sharp peaks above background and that of amorphous broad peak that is the area under the smooth curve above background, respectively. The degree of crystallization was estimated by using JADE 6.0 (Materials Data, Inc.). The degree of crystallization estimated here has a large margin of error because it is difficult to plausibly approximate a background curve. The obtained data are summarized in Table 3.

4. Results

4.1 Sequential extraction of major elements in Japanese geochemical reference materials

Figure 1 shows the distribution of Al, P, Na, K, Mg, Ca, Mn, and Fe concentrations in samples for four fractions obtained by the BCR scheme (Table 2). We explain the distribution of elements in the geochemical reference materials in a straightforward manner because Kubota *et al*. (2014) carefully explained the method in which the speciation of elements extracted by the BCR protocol reflects their origins or sedimentation environments. Essentially, step 4, the final residue step, is the most dominant fraction for all elements except for Mn. The Ca is strongly extracted in step 1; P and Fe are removed in step 2; and Mn is abundantly extracted in steps 1 and 2. The high percentages of P, Mn, and Fe extracted in step 2 are explained by the iron– manganese (hydro–) oxide phase. The high proportions of Na and K in JSd-4, JMs-1, and JMs-2 extracted in step 1 are explained by sea salt contamination because marine sediments were not desalinated (Terashima *et al.*, 2002; Kubota *et al*., 2014). The high percentages of Ca and Mg in step 1 for JSd-4, JMs-1, and JMs-2 indicate the digestion of calcium carbonate. Al in JSO-1 is strongly extracted in steps 2 and 3. This fact indicates that JSO-1 is abundant in amorphous aluminum–iron hydroxide and in Al bound to organic material. Fe in JSd-2 is expected to be highly extracted in step 3 of the process because it is originated from metamorphic rocks associated with the Hitachi copper mine (Omori *et al*., 1986). However, the proportion of Fe in JSd-2 was higher in the step 2 extraction at approximately 20 % but was lower in step 3 at 10 % (Fig. 1). Kubota *et al*. (2014) assumed that pyrite may have been oxidized to iron hydroxide or that the relative abundance ratio of pyrite to crystalline minerals containing Fe would be small.

Table 3 Degree of crystallization (%) of geochemical reference materials

Name	Untreated	Step 1*	Step 2*	Step 3*
JLk-1	39%	40%	40%	41%
JSO-1	13%	17%	16%	24%
JSd-1	65%	68%	69%	69%
JSd-2	63%	66%	68%	66%
JSd-3	67%	71%	71%	72%
JSd-4	36%	41%	44%	47%
JMs-1	40%	42%	45%	47%
JMs-2	28%	29%	36%	35%

* Steps 1, 2, and 3 represent the residues of the samples after steps 1, 2, and 3 of the extraction, respectively. Degree of crystallization (%) was estimated within the range of 10–40° (2θ) after back ground removal.

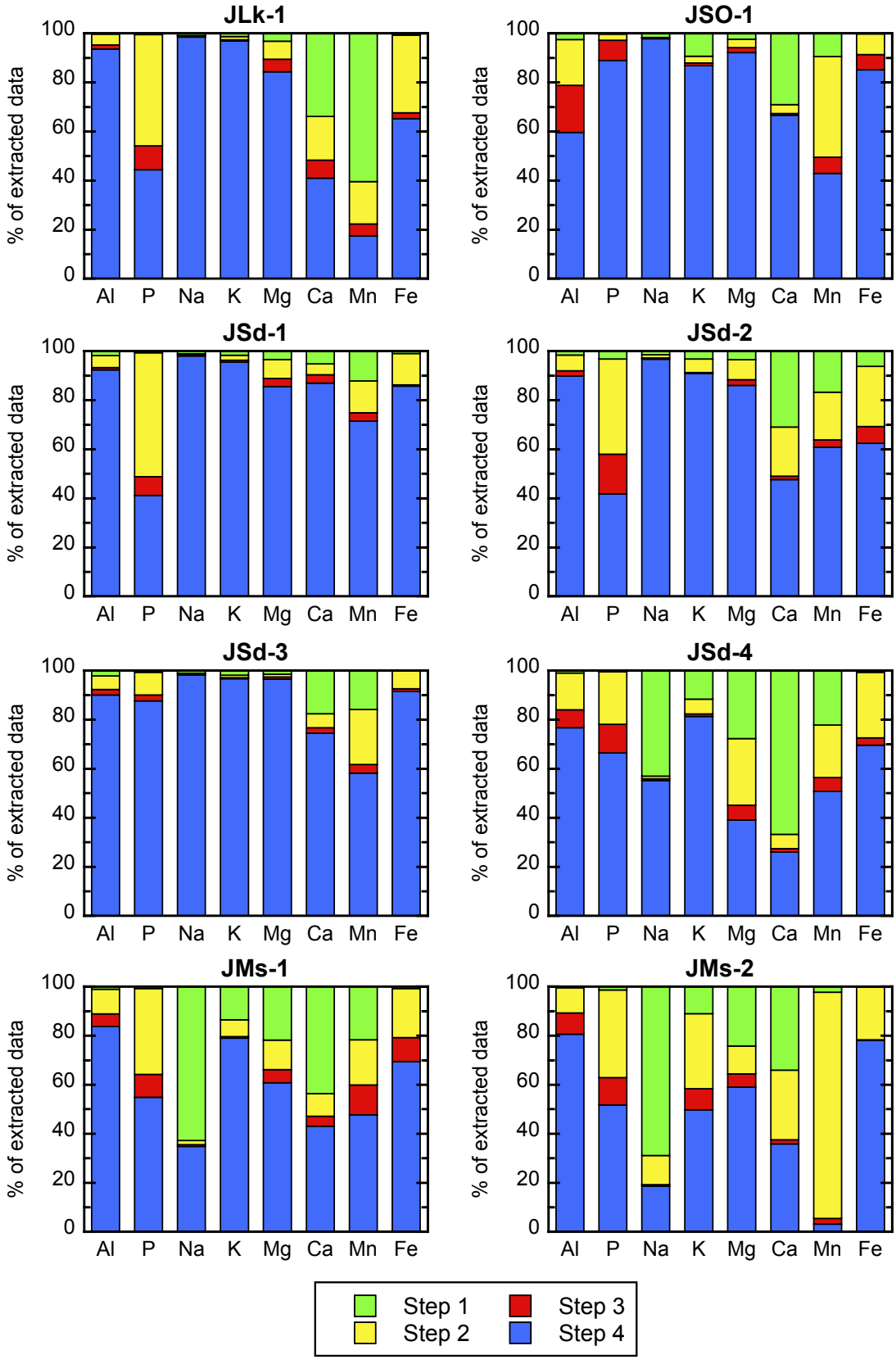

Fig. 1 Distribution of Al, P, Na, K, Mg, Ca, Mn, and Fe concentrations in geochemical reference materials for four the fractions obtained by the Community Bureau of Reference (BCR) scheme. The data were obtained from Kubota *et al*. (2014).

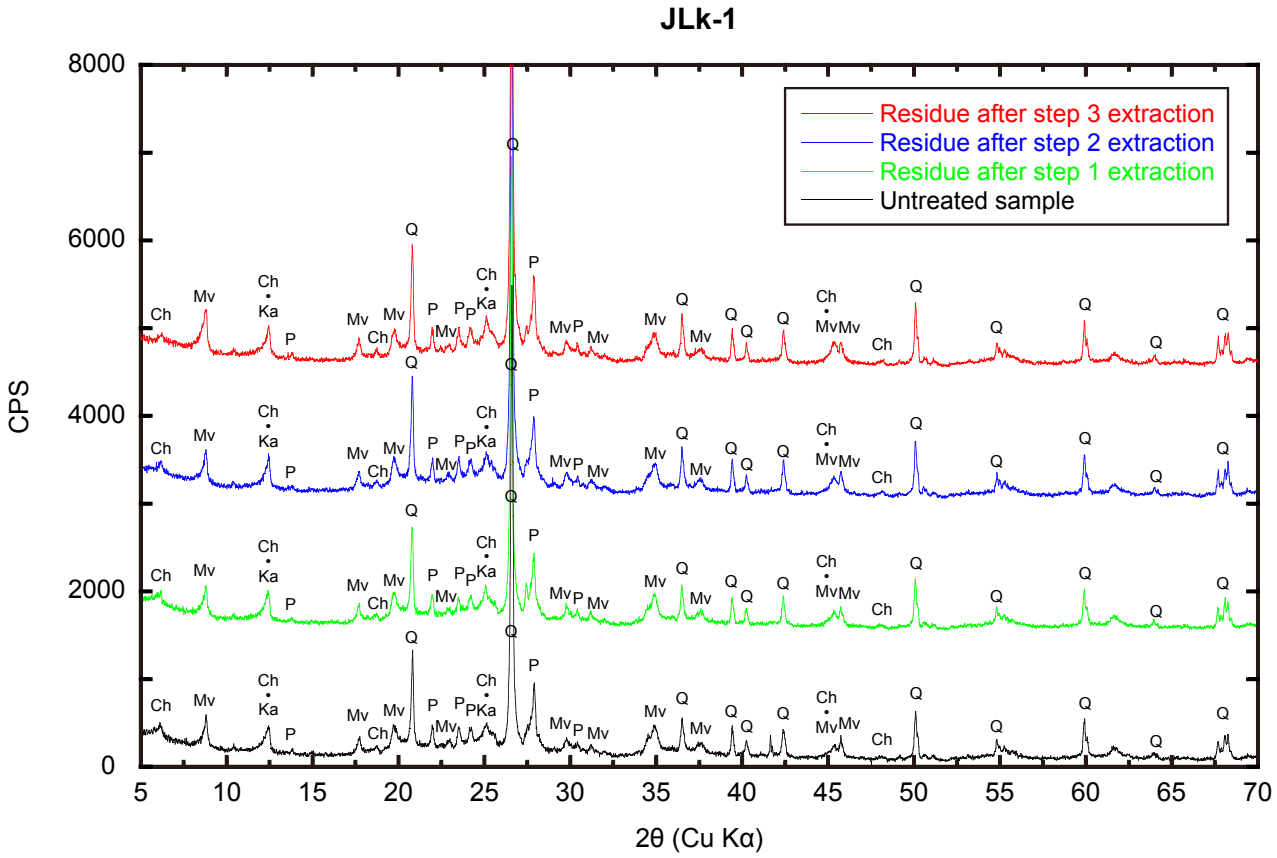

Fig. 2 X-ray diffractometry (XRD) patterns of JLk-1.
Q: quartz, P: plagioclase, K: K-feldspar, Mv: muscovite, Ch: chlorite, Ka: kaolinite.

4.2 XRD patterns of untreated samples and residue of samples after sequential extraction

Figures 2–5 show XRD patterns of samples with no treatment and the residue of those after steps 1–3 of the extraction. The XRD peaks of calcite, gypsum, and halite in JMs-1, JMs-2, and JSd-4 disappeared after step 1 of the extraction; that of pyrite in JMs-1 disappeared after step 3. The intensities of XRD peaks of quartz and plagioclase in JSO-1 increased after the third extraction procedure. For JLk-1, JMs-1, JSd-1–4, the intensities of XRD peaks of chlorite, kaolinite, and muscovite, which are clay and mica minerals, did not change after steps 1, 2, and 3. The fact suggests that following BCR protocol does not result in damage to these fragile minerals. It is expected that the decomposition of the iron–manganese (hydro–) oxide phase at step 2 of the extraction elevates the degree of crystallization; nevertheless, the value scarcely changed except for the case of JMs-2 (Table 3). In addition, the diffraction peaks of magnetite and hematite in JSO-1, JMs-1, JSd-1, JSd-2, and JSd-4, which are iron oxide minerals, did not change during the sequential extraction procedure.

5. Discussion

5.1. JLk-1

The diffraction peaks of quartz, plagioclase, muscovite, chlorite, and kaolinite were recognized in the untreated JLk-1 sample. The peak intensities of these minerals scarcely changed after steps 1, 2, and 3 of the extraction procedures. The JLk-1 sample is characterized by high extraction percentages of Ca and Mn in step 1 and those of Fe and P in step 2 (Fig. 1). It is known that the surface sediments of Lake Biwa are highly enriched in P, Mn, Ni, Cu, Zn, As, Cd, and Pb as a result of early diagenetic processes (Kobayashi *et al*., 1975; Nakashima, 1982). The Ca and Mn in the step 1 are assumed to exist as an exchangeable phase (Kubota *et al.*, 2014), which cannot be detected through XRD. More than 30 % of the Fe in JLk-1 was extracted in step 2; however, a significant increase in the degree of crystallization percentage was not evident after this step. The value, 39 % – 41 %, was nearly constant during the sequential extraction procedure. In addition, the degree of crystallization was relatively lower in this sample than that in JSd-1–4 and

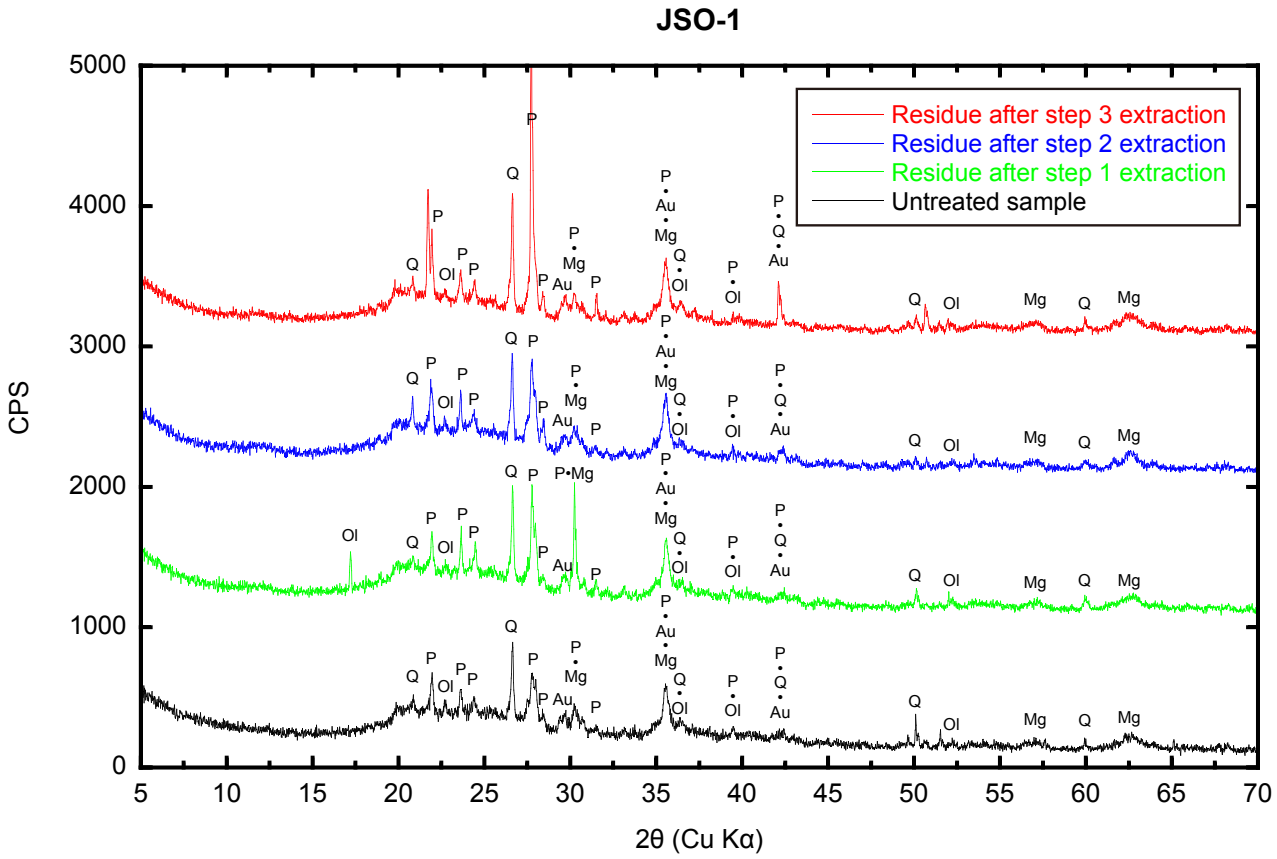

Fig. 3 X-ray diffractometry (XRD) patterns of JSO-1.
Q: quartz, P: plagioclase, Au: augite, Ol: olivine, Mg: magnetite.

JMs-1. This fact may indicate that the amorphous phase in JLk-1 is composed dominantly of opal diatoms that were not decomposed during the sequential extraction procedure. The presence of such diatoms was previously reported by Ando *et al*. (1990).

5.2. JSO-1

The XRD patterns of untreated JSO-1 presented small peaks of plagioclase, quartz, olivine, augite, and magnetite (Fig. 3). The presence of olivine and augite imply the influence of volcanic materials (Terashima *et al*., 2002). The amorphous halo pattern was characteristic in this sample. Although Terashima *et al*. (2002) suggested that allophane, a non-crystalline hydrous aluminosilicate, is the most dominant species in JSO-1, volcanic glassy material was present as a rather minor species. Such amorphous materials are not intended to be decomposed during the BCR procedure. Table 3 indicates that the degree of crystallization increases significantly after the step 3 extraction procedure. Such a significant increase was detected for only JSO-1. Thus, the increase of the degree of crystallization relates to decomposition of organic matter. JSO-1 is highly enriched in organic matter. At 8.91 %, the total C concentration in JSO-1 was much higher than that in the other samples (Table 1). The XRD patterns show that the peak intensities of quartz and plagioclase increased significantly after step 3. We assumed that organic matter thickly covering the crystalline minerals reduced the reflection intensity from those materials. Kodama (1995) reported that a mineral surface coated with an amorphos substance in soil material provides an amorphous halo with less intensive peaks in the XRD patterns. After extraction of the amorphous material from soil by using sequential extraction methods, its XRD peaks were those of disinct minerals (Kodama, 1995). That is, the changes in the XRD patterns after the step 3 were caused by decomposition of organic material on the mineral surfaces.

5.3. JMs-1 and JMs-2

The XRD patterns of untreated JMs-1 contain quartz, plagioclase, chlorite, mica, pyrite, halite, calcite, and gypsum (Fig. 4a). The XRD peaks of halite, calcite, and gypsum disap-

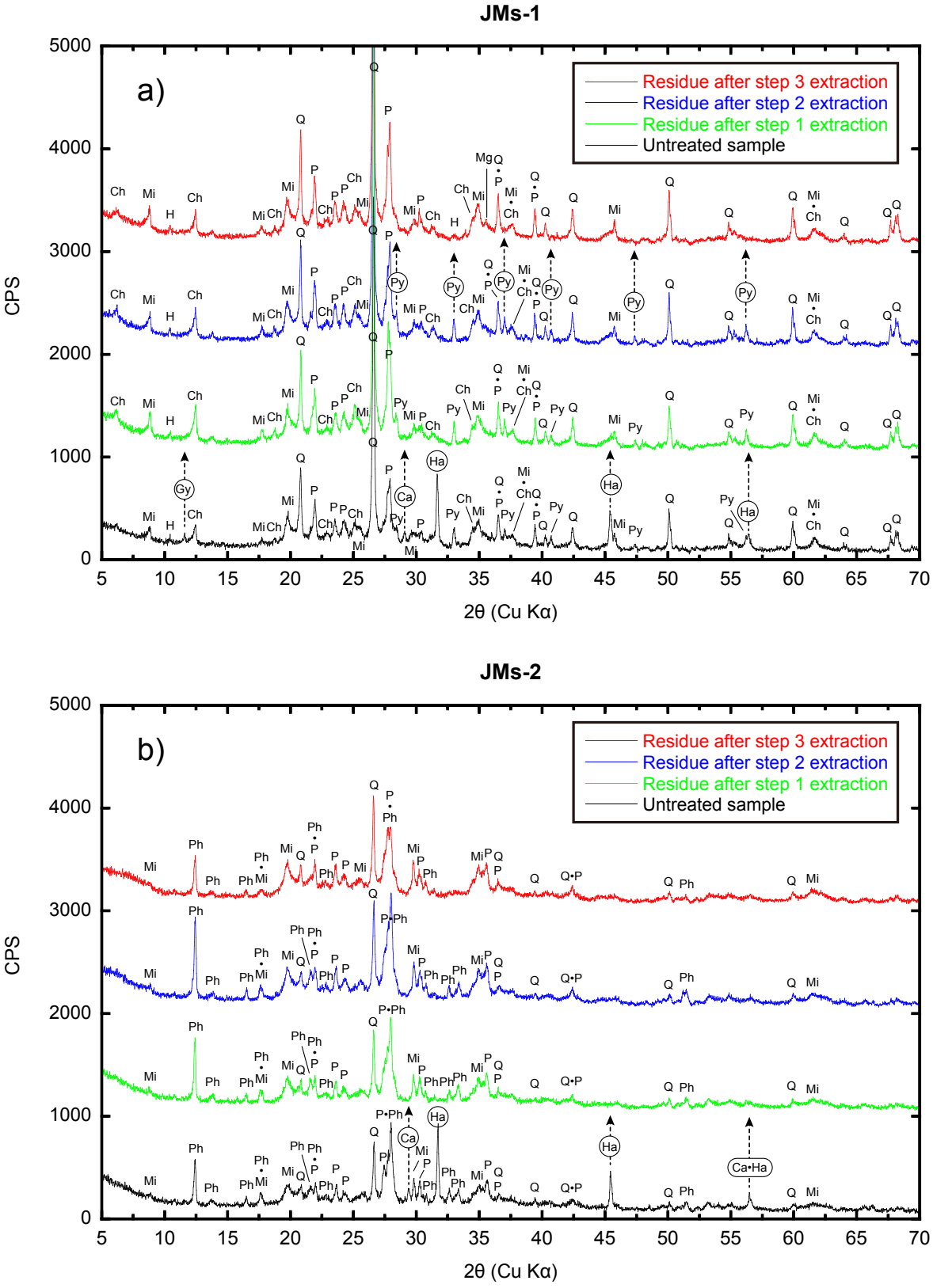

Fig. 4 X-ray diffractometry (XRD) patterns of JMs-1 and JMs-2. Q: quartz, P: plagioclase, H: hornblende, Mi: mica, Ph: phillipsite, Ch: chlorite, Ca: calcite, Py: pyrite, Mg: magnetite, Gy: gypsum. Circle and dashed arrow indicate that the mineral has been decomposed by the sequential extraction procedure.

peared after step 1 of the extraction. Halite and gypsum were crystallized from sea salt during the drying process because JMs-1 was not desalinated. This feature corresponds to the high proportions of Na, K, Mg, and Ca extracted in step 1 (Fig. 1). JMs-1 has a high Cl concentration of 2.69 % (Table 1). Considering the total Cl percentage originated from sea salt, the Na concentration in the halite (NaCl) was calculated to be 1.74 %, which corresponds to the 1.86 % Na extracted in step 1 (Table 2). 10 % of the total Fe was extracted in step 3; this percentage is the highest among those of the geochemical reference materials (Fig. 1). Accordingly, the XRD peaks of pyrite disappeared after step 3. BCR procedures successfully decomposed sulfide in step 3. The pyrite in JMs-1 should be an authigenic phase because Tokyo Bay frequently becomes a dysoxic environment; Terashima *et al.* (2002) reported that the collected sediment had mostly anoxic facies. JMs-1 has a high total S concentration of 1.32 % (Table 1). Considering that the Fe extracted in step 3 was composed of only pyrite, which is not an organic phase, the S concentration of the pyrite phase is estimated to be 0.51 %. This value is significantly smaller than the total S concentration. The sulfate minerals such as gypsum and the organic materials could be the dominant sources of S in JMs-1.

Figure 4b shows that phillipsite is the dominant mineral of JMs-2. Quartz, plagioclase, and mica appeared slightly in the XRD patterns (Fig. 4b). JMs-2 contains a large amount of amorphous material such as basaltic hyaloclastite (volcanic glass), aluminum hydroxide, and opal (Terashima *et al*., 2002), which explains the lower than 50 % degree of crystallization (Table 3). Considering that the Na and Ca extracted in step 1 originated from halite and calcite, the concentrations of Cl in halite and C in calcite were calculated to be 4.14 % and 0.32 %, respectively. These values correspond to the concentrations of total Cl (4.05 %) and C (0.39 %) in JMs-2 (Table 2). Therefore, the contribution of organic material to the C concentration was very small. In addition, the total S concentration was low at 0.29 % (Table 1). Therefore, it is expected that the concentrations of elements extracted in step 3 are also low. However, Kubota *et al*. (2014) reported that non-negligible amounts of Al, K, and Rb in JMs-2 were extracted in step 3, which is a characteristic feature of JMs-2. Accordingly, the peak intensities of phillipsite at 12.4° and 27.9° (2θ) weakened after step 3 of the extraction. In that process, the samples were reacted with H_2O_2 at room temperature for 1 h and were then heated at 85 °C for 1 h (Rauret *et al*., 1999). Marine phillipsite, belonging to a zeolite group, formed from hyaloclastite and is highly enriched in K (e.g., Sheppard *et al*., 1970). Therefore, phillipsite would be partly decomposed in this process.

Figure 1 shows that Na, Mg, P, K, Ca, Mn, and Fe in JMs-2 were strongly extracted in step 2 ; an extremely high proportion of Mn, 92 %, was extracted in this process (Kubota *et al*., 2014). The Na, Mg, K, and Ca extracted in step 2 would be incorporated into the Mn dioxide (e.g., Moorby *et al*., 1984). The degree of crystallization of JMs-2 increased significantly after that step (Table 3), which may indicate that amorphous iron hydroxide and manganese dioxide were decomposed in step 2. Although such a large increase in the degree of crystallization was not detected in the other geochemical reference materials, 10 % – 30 % of the total Fe was extracted in step 2 for all samples (Fig. 1). The amounts of crystalline materials such as quartz and plagioclase were small in JMs-2 (Fig. 4b). Therefore, the relative ratios by weight of iron hydroxide and manganese dioxide in JMs-2 would be much larger than those in JLk-1, JSd-1–4, and JMs-1.

5.4. JSd-1–4

JSd-1 is stream sediment originating from granitic rocks. Quartz, plagioclase, K-feldspar, hornblende, biotite, kaolinite, and magnetite were recognized in its XRD patterns (Fig. 5a). The peak intensities of respective minerals did not change after the sequential extraction procedure. This fact corresponds to the low extraction ratios in steps 1–3 for major elements according to BCR protocol (Fig. 1).

JSd-2 is composed of stream sediment collected from a drainage basin containing high-temperature metamorphic rocks (Hitachi metamorphic rock) and those from Hitachi Cu mine. The XRD patterns of the untreated JSd-2 sample showed quartz, plagioclase, K-feldspar, chlorite, hornblende, muscovite, epidote, calcite, and magnetite (Fig. 5b). The chlorite, hornblende, muscovite, epidote, and calcite correspond to mineralogical compositions of Hitachi metamorphic rock (Omori *et al*., 1986). The calcite, which showed a very weak peak in the XRD patterns of the untreated sample at $2\theta = 29.4°$, disappeared after step 1 of the extraction. The Hitachi Cu mine yields pyrite and chalcopyrite as dominant ore deposits. The high concentration of S at 1.32 % (Table 1) in JSd-2 may indicate the inputs of these sulfide minerals. However, the XRD patterns of JSd-2 showed no distinct diffraction peaks of chalcopyrite. The 1100 mg/kg of Cu in JSd-2 (Terashima *et al*., 1990) would be too low to be visible in the XRD patterns even if the total Cu exists as chalcopyrite. Moreover, the existence of pyrite is difficult to be recognized in the XRD chart because the dominant peaks attributed to this mineral were superimposed by those of other minerals such as plagioclase, hornblende, and epidote. Very weak X-ray intensities of pyrite were scarcely observed at 37.1°, 40.7°, and 47.4° (2θ); the peaks at 40.7° and 47.4° (2θ) seemed to disappear after step 3. The concentration of Fe extracted in step 3 of JSd-2 was 0.59 %, which is higher

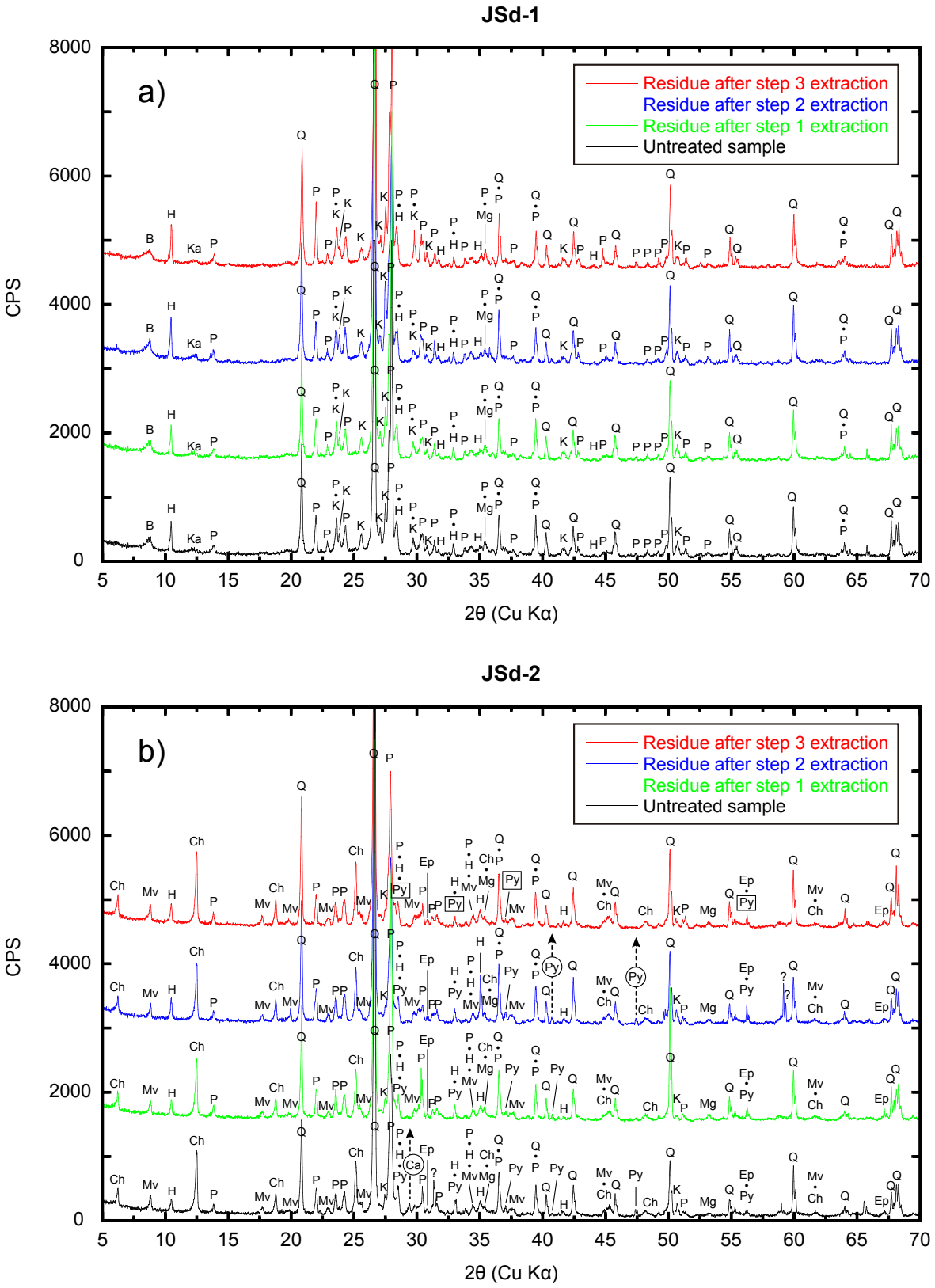

Fig. 5 a), b) X-ray diffractometry (XRD) patterns of JSd-1–4. Q: quartz, P: plagioclase, K: K-feldspar, H: hornblende, Au: augite, B: biotite, Mv: muscovite, Ch: chlorite, Ka: kaolinite, Ep: epidote, Ca: calcite, Py: pyrite, Hm: hematite, Mg: magnetite, Gy: gypsum, Un: unknown material. Circle and dashed arrow indicate that the mineral has been decomposed by the sequential extraction procedure. Square indicates that the peaks related to pyrite did not disappear after step 3 of the extraction.

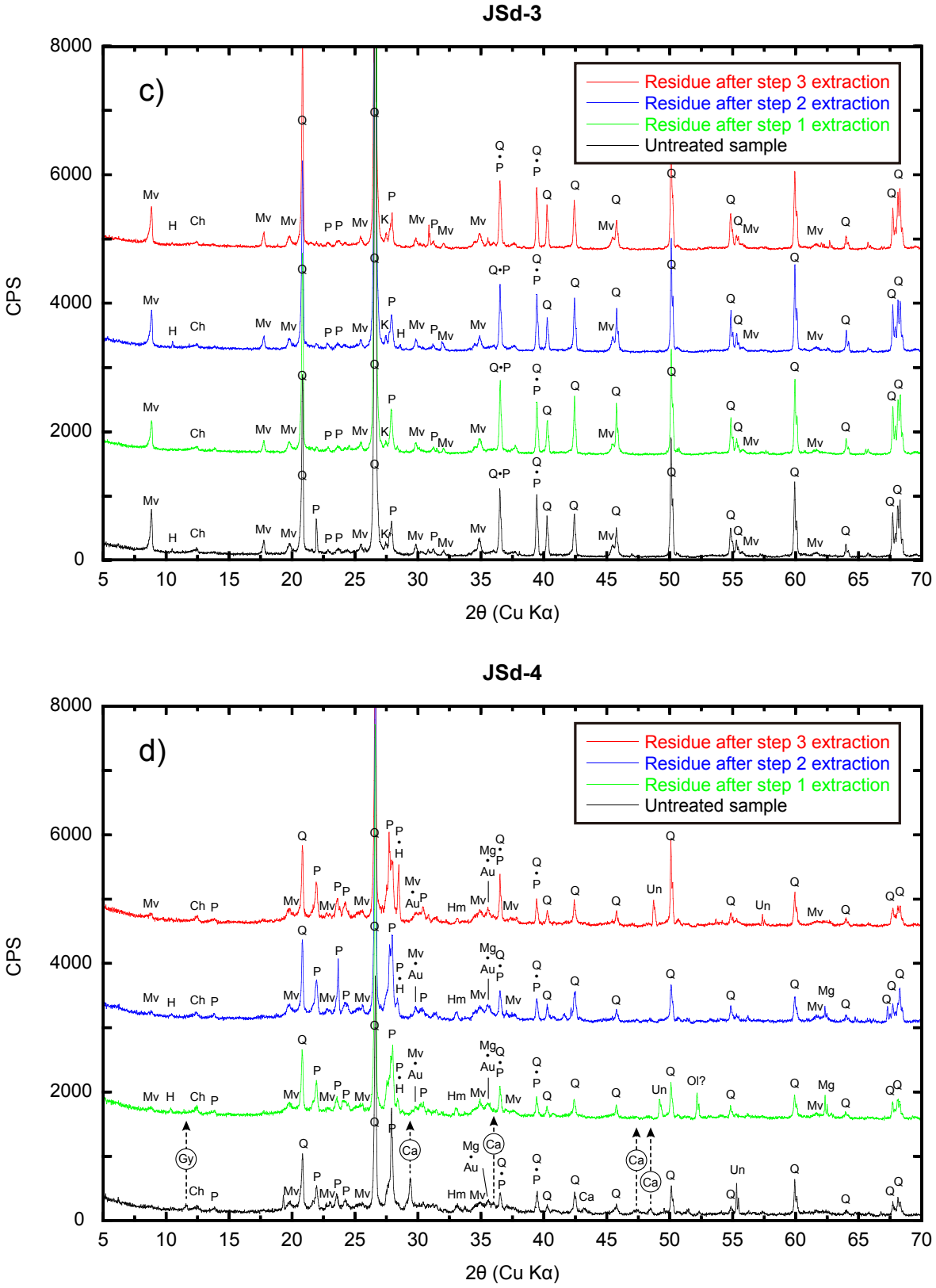

Fig. 5 c), d) X-ray diffractometry (XRD) patterns of JSd-1–4. Q: quartz, P: plagioclase, K: K-feldspar, H: hornblende, Au: augite, B: biotite, Mv: muscovite, Ch: chlorite, Ka: kaolinite, Ep: epidote, Ca: calcite, Py: pyrite, Hm: hematite, Mg: magnetite, Gy: gypsum, Un: unknown material. Circle and dashed arrow indicate that the mineral has been decomposed by the sequential extraction procedure.

than that of JMs-1 at 0.44 % (Table 2); however, the relative abundance ratio of Fe extracted in step 3 to the total Fe was only 8 % (Fig. 1). Although pyrite is a minor mineral in JSd-2, it seemed to be decomposed in step 3 extraction processes. The low content of pyrite is attributed to its oxidation to iron hydroxide during the weathering process or to dilution by the input of the other minerals enriched in Fe such as chlorite, hornblende, and epidote, as suggested by Kubota *et al*. (2014).

JSd-3 is composed of stream sediment derived from mélange matrix and chert blocks of accretionary complexes distributed in the central part of Ibaraki Prefecture. A very intensive peak of quartz in the XRD pattern may represent origins of sandy sediments or chert of accretionary complexes distributed near the sampling location (Fig. 5c). Muscovite, plagioclase, K-feldspar, and chlorite were also recognized (Fig. 5c). No systematic changes after the sequential extraction procedure was detected in the XRD patterns, as was the case for JSd-1. The extraction ratios of major elements at steps 1–3 according to the BCR protocol were also very low (Fig. 1).

JSd-4 was collected from an urban river flowing through an alluvial plain in Kanto Plain. The XRD patterns of the untreated bulk sample showed quartz, plagioclase, muscovite, chlorite, hornblende, augite, hematite, calcite, and gypsum (Fig. 5d). This sample is characterized by a lower degree of crystallization than that in JSd-1–3. Kubota *et al*. (2014) assumed that the high percentages of Na, Mg, K, and Ca extracted in step 1 could be explained by the digestion of sea salt and calcium carbonate (Fig. 1). However, halite was not recognized in the XRD patterns. The concentrations of Na and K extracted in step 1 for JSd-4 were lower than those of JMs-1 and JMs-2 (Table 2). The concentrations of Mg and Ca extracted in step 1 for these reference materials showed opposite characteristics (Table 2). Table 2 also shows the data of stream sediment (no. 25023) collected from the estuarine region in Osaka Plain; however, this sample was contaminated by sea salt (Ohta *et al*., 2007). The concentrations of Na, Mg, K, and Ca extracted in step 1 of no. 25023 correspond to those of the JMs-1 well. Therefore, it is concluded that JSd-4 was not influenced by sea salt. Nevertheless, a distinct peak of calcite and a small peak of gypsum were detected in the XRD patterns of the untreated sample, which both disappeared after step 1 of the extraction. JSd-4 did not contain biogenic carbonates such as coral or shell fragments. Such conflicting results can be explained by contamination by cement fragments. Cement is used everywhere in urban areas, and urban streams flow through concrete embankments. The Japan Cement Association (http://www.jcassoc.or.jp/, accessed March 19, 2014.) has defined cement as being composed of calcite, gypsum, and aggregates such as a river or sea gravel. Therefore, the high extraction percentages of Ca in step 1 and the presence of calcite and gypsum in the untreated sample can be attributed to contamination by cement materials. However, Na and K are not abundant in cement because they accelerate its deterioration. Magnesium is also not abundant in cement. These elements may have been simply absorbed onto the mineral surfaces without crystallization because they exist as an exchangeable phase. Alternatively, Kubota *et al*. (2014) reported that JSd-4 is contaminated by industrial slag material because it consists of oxides of Mg, Al, Si, Ca, Na, and K and has been widely used for construction materials such as cement, soil stabilizer, road pavement, and building brick (e.g., Nagano *et al*., 2007; Nishi and Kawabata, 1990). In particular, the high percentages of Na, Mg, and K extracted in step 1 may be explained by construction materials including slag. Slowly cooled slag is composed of gehlenite ($Ca_2Al_2SiO_7$), åkermanite ($Ca_2MgSi_2O_7$), wollastonite ($CaSiO_3$), and dicalcium silicate ($2CaO{\cdot}SiO_2$) (Nishi and Kawabata, 1990). However, XRD peaks of those minerals were not observed for JSd-4. It is possible that JSd-4 contains granulated slag of which hypercalcified aluminosilicate glass (amorphous phase) is the dominant phase (Nishi and Kawabata, 1990). In this regard, the lower degrees of crystallization of JSd-4 than those of JSd-1–3 may be attributed to contamination by industrial slag. Eto and Yamamoto (2002) examined the origin of riverbed sediments (mainly gravels) collected from the Katabira River flowing in Yokohama City, which is an urban river. They detected a maximum of 27 % of artificial gravel in the riverbed that was composed predominantly of concrete and brick fragments. Therefore, although Eto and Yamamoto (2002) examined gravels rather than fine sediments, our assumption that JSd-4 contains cement and slag materials is reasonable.

6. Summary

We have examined the manner in which the mineralogical composition of Japanese geochemical reference materials changes by application of the sequential extraction procedure. This procedure, developed by the BCR, decomposes and extracts exchangeable and carbonate phases in the first step (step 1), iron hydroxide and manganese oxide in the second step (step 2), and metal sulfide and organic material in the third step (step 3). Calcite, halite, and gypsum were decomposed satisfactorily in step 1 extraction; pyrite was decomposed in step 3 of the extraction. These results are comparable to those of respective target phases. In contrast, it was difficult to determine whether iron hydroxide and manganese oxide were decomposed in step 2 of the extraction because these materials did not show distinct peaks in the XRD patterns, unlike those

exhibited by the other minerals. Essentially, XRD peak intensities of crystalline minerals did not change significantly after the sequential extraction procedure. One exception, phillipsite in JMs-2, was partially decomposed in step 3. Moreover, the peak intensities of quartz and plagioclase in JSO-1 increased after that step. These results indicate that organic material was removed totally by the third extraction procedure because organic materials covering the mineral surfaces reduced the X-ray reflections of the minerals.

Acknowledgments: The authors are grateful to Masaya Suzuki for his technical support in the XRD measurement.

References

Ando, A., Okai, T., Inouchi, Y., Igarashi, T., Sudo, S., Marumo, K., Itoh, S. and Terashima, S. (1990) JLs-1 and JDo-1, GSJ rock reference samples of the "Sedimentary rock series" *Bull. Geol. Surv. Japan*, **41**, 27-48.

Crosland, A. R., McGrath, S. P. and Lane, P. W. (1993) An inter-laboratory comparison of a standardized EDTA extraction procedure for the analysis of available trace-elements in two quality-control soils. *Int. J. Environ. Anal. Chem*., **51**, 153-160.

Coetzee, P. P., Gouws, K., Plüddemann, S., Yacoby, M., Howell. S. and den Drijver, L. (1995) Evaluation of sequential extraction procedures for metal speciation in model sediments. *Wat. SA*., **21**, 51–60.

Darnley, A. G., Björklund, A., Bølviken, B., Gustavsson, N., Koval, P. V., Plant, J. A., Steenfelt, A., Tauchid, M., Xie, X., Garrett, R. G. and Hall, G. E. M. (1995) *A global geochemical database for environmental and resource management: recommendations for international geochemical mapping.* UNESCO Publishing, Paris, 122 pp.

Eto, T. and Yamamoto, S. (2002) Origin of riverbed sediments in the River Katabira in Yokohama, central Japan. *Journal of the Faculty of Education and Human Sciences, Yokohama National University. The natural sciences,* **4**, 25-38 (In Japanese with English abstract).

Imai, N., Terashima, S., Ohta, A., Mikoshiba, M., Okai, T., Tachibana, Y., Togashi, S., Matsuhisa, Y., Kanai, Y. and Kamioka, H. (2004) *Geochemical map of Japan*. Geological Survey of Japan, AIST, 209 pp (In Japanese with English abstract).

Imai, N., Terashima, S., Itoh, S. and Ando, A. (1996) 1996 compilation of analytical data on nine GSJ geochemical reference samples, ''Sedimentary rock series''. *Geostand. Newsl*., **20**, 165-216.

Imai, N., Terashima, S., Ohta, A., Mikoshiba, M., Okai, T., Tachibana, Y., Togashi, S., Matsuhisa, Y., Kanai, Y. and Kamioka, H. (2010) Elemental distribution in Japan -Geochemical map of Japan-. (Imai, N., ed.). *Geological Survey of Japan*, AIST, Tsukuba (In Japanese with English abstract).

Kobayashi, J., Muramoto, S., Nakashima, S., Teraoka, H. and Horie, S. (1975) Distribution of arsenic, cadmium, lead, zinc, copper, and manganese contained in the bottom sediment of Lake Biwa. *Jap. J. Limnol*., **36**, 6-15 (In Japanese with English abstract).

Kodama, H. (1995) Identificationand quantification of non-crystalline inorganic materials in soils by selective chemical dissolution method. *Chishitsu News*, **496**, 26-35 (In Japanese).

Kubota, R. (2009) Simultaneous determination of total carbon, nitrogen, hydrogen and sulfur in twenty–seven geological reference materials by elemental analyser. *Geostand. Geoanal. Res*., **31**, 271-283.

Kubota, R., Ohta, A. and Okai, T. (2014) Speciation of 38 elements in eight Japanese geochemical reference materials sediments series determined using sequential extraction technique. *Geochem. J*., **48**, 165-188.

Martin, J. M., Nirel, P. and Thomas, A. J. (1987) Sequential extraction techniques: Promises and problems. *Mar. Chem*., **22**, 313–341.

Moorby, S. A., Cronan, D. S. and Glasby, G. P. (1984) Geochemistry of hydrothermal Mn-oxide deposits from the S.W. Pacific island arc. *Geochim. Cosmochim. Acta*, **48**, 433-441.

Nagano, N., Takahashi, T., Tomita, K., Wakasugi, M., Kudo, K. and Omote, R. (2007) Study on chemical properties of molten slag derived from municipal solid waste. *Reports of the Hokkaido Industrial Research Institute*, **306**, 47-53 (In Japanese with English abstract).

Nakashima, S. (1982) Partitioning of heavy metals (Mn, Fe, As, Cd, Pb, Cu, Zn, Co and Ni) into selective chemical fractions in sediment cores from Lake Biwa. *Jap. J. Limnol*., **43**, 67-80 (In Japanese with English abstract).

Nishi, M. and Kawabata, K. (1990) Some basic and mechanical properties of iron and steel slags as base-course materials. *Journal of geological engineering*, **414**, 89-98 (In Japanese with English abstract).

Nishimura, A. and Saito, Y. (1994) Deep-sea sediments in the Penrhyn Basin, South Pacific (GH 83-3 area). In: Usui, A. (Ed.), *Geological Survey of Japan Cruise Report* **23**, Geol. Surv. Japan, Tsukuba, pp. 41-60.

Ohta, A., Imai, N., Terashima, S. and Tachibana, Y. (2007) Preliminary study for speciation geochemical mapping using a sequential extraction method. *Bull. Geol. Surv. Japan*, **58**, 201-237.

Omori, M., Hayama, Y. and Horiguchi, M. (1986) *Regional Geology of Japan. Part 3 (KANTO)*. Kyoritsu Shuppan Co., 350 pp (In Japanese).

Rauret, G., López-Sánchez, J. F., Sahuquillo, A., Rubio, R., Davidson, C., Ure, A. and Quevauviller, P. (1999) Improvement of the BCR three step sequential extraction procedure prior to the certification of new sediment and soil reference materials. *J. Environ. Monit*., **1**, 57-61.

Sheppard, R. A., Gude, A. J. and Griffin, J. J. (1970) Chemical composition and physical propertibs of phillipsite from the Pacific and Indian Ocean. *Am. Mineral*., **55**, 2053-2062.

Sutherland, R. A. (2010) BCR®-701: A review of 10-years of sequential extraction analyses. *Anal. Chim. Acta*, **680**, 10-20.

Terashima, S., Ando, A., Okai, T., Kanai, Y., Taniguchi, M., Takizawa, F. and Itoh, S. (1990) Elemental concentrations in 9 new GSJ rock reference samples sedimentary-rock series. *Geostand. Newsl*., **14**, 1-5.

Terashima, S., Imai, N., Taniguchi, M., Okai, T. and Nishimura, A. (2002) The preparation and preliminary characterisation of four new Geological Survey of Japan geochemical reference materials: Soils, JSO-1 and JSO-2; and marine sediments, JMS-1 and JMS-2. *Geostand. Newsl.*, **26**, 85-94.

Ure, A. M., Quevauviller, P., Muntau, H. and Griepink, B. (1993) Speciation of heavy-metals in soils and sediments - an account of the improvement and harmonization of extraction techniques undertaken under the auspices of the BCR of the commission-of-the-European-communities. *Int. J. Environ. Anal. Chem*., **51**, 135-151.

Received March 13, 2014
Accepted June 30, 2014

地球化学標準物質（堆積物シリーズ）に逐次溶解法を適用した際に生じる鉱物組成変動

太田充恒・久保田蘭・岡井貴司

要　旨

我々は Community Bureau of Reference（BCR)によって確立された逐次溶解法を, 8 つの日本の地球化学標準物質へ適用することを試みた. この方法は, step 1 で交換態･炭酸塩態, step 2 で鉄水酸化物態･マンガン酸化物態, step 3 で金属硫化物態･有機物態をそれぞれ分解抽出する事を目的としている.本研究では,未処理の試料と各stepで抽出作業を行った後の残渣試料に対してX線回折（XRD）パターンを調べることで,抽出目的相が適切に分解されているかを確認することを目的とした. JSd-1 とJSd-3 に対してBCR法を適用した際, XRDパターンには有意な変化は認められなかった. この結果は,これらの物質に含まれる元素の多くがBCR法によってほとんど抽出されなかった事実と調和的である. これに対し, JSd-4, JMs-1, JMs-2 に含まれる方解石由来のピークは step 1 適用後にXRDパターンから全て消滅した. この結果は, step 1の目的相が十分に分解されたことを示す. JLk-1 や JMs-2 では,高い濃度の鉄とマンガンが step 2 で抽出される. しかし, 鉄水酸化物態･マンガン酸化物は明瞭なピークをXRDパターンに示さないため, これらの物質が step 2 で十分に分解されたかどうかを明らかにすることは困難であった. 一方, JMs-1 中のパイライトのピークが step 3 抽出後に消滅した事から,硫化物がこの過程で適切に分解される事が明らかとなった. また, JSO-1 において, step 3 抽出後に石英や斜長石のピーク強度（X線回折強度）が大きく増加することが認められた. step 3 以前では有機物が鉱物表面を厚く覆っているために, 鉱物からのX線回折強度を下げていたためと推測された. 従って,間接的な証拠であるものの, step 3 抽出手順において有機物が適切に分解除去されたと言える. これらの結果より, BCR法によって地球化学標準物質から目的物質を適切に分離抽出することが可能であることが確認された.